BOUNDARY LAYER CONTROL AS A METHOD
OF GAS TURBINE BLADE COOLING

A THESIS

Submitted to the Graduate Faculty
of the
University of Minnesota

by
DWIGHT C.sten NESS
COMDR. U.S.N.

In Partial Fulfillment of the Requirements
for the
Degree of Master of Science
in
Aeronautical Engineering

August
1949

ACKNOWLEDGMENTS

The author wishes to express his sincere appreciation to the following who aided in this study:

Professors B. J. Robertson, N. A. Hall, T. E. Murphy, and K. E. Neumeier of the Mechanical Engineering Department, for their assistance, advice and suggestions.

Shop personnel of the Oak Street Laboratory for their assistance in construction of the test equipment.

TABLE OF CONTENTS

INDEX OF TABLES AND FIGURES

TABLES

FIGURES

OBJECT AND SCOPE

The object of this thesis was to determine the feasibility of cooling gas turbine blades by introduction of a controlled boundary layer of cool air over the blade surface.

This investigation included a static test of a single instrumented turbine blade in a variable high velocity, high temperature gas stream with variable cooling air flow. Two configurations of the test blade were used to produce variation in boundary layer control.

INTRODUCTION

Maximum effort in the development of gas turbines is being exerted to improve specific power output, to reduce specific fuel consumption and to increase reliability. The most promising field for the attainment of these objectives lies in increasing the turbine inlet temperature which is presently limited by permissible operating temperatures of blading materials. An investigation of the gas turbine thermodynamic cycle reveals the magnitude of improvement possible by increasing turbine operating temperatures. Such an investigation conducted by the NACA (Ref. 1) shows that for a given mass flow of working fluid the specific power output is proportional and the specific fuel consumption is inversely proportional to the inlet temperature. Fig. 1 illustrates this relation.

The increase of turbine inlet temperature, however, is limited by high temperature strength of blade materials. The development of high temperature metals is proceeding, but at a slow rate. How slowly metallurgical progress has been made is shown in Fig. 83 of Ref. 2. Allowable blade temperatures advanced from 1180° F. in 1935 to 1200° F. by 1940 and to 1385° F. by 1945. The rate of increase has been no greater since 1945.

Non-metallic materials such as ceramics have yet to demonstrate their adaptability to the rigorous service

INTRODUCTION

Maximum effort in the development of gas turbines is being exerted to improve specific power output, to reduce specific fuel consumption and to increase reliability. The most promising field for the attainment of these objectives lies in increasing the turbine inlet temperature which is presently limited by permissible operating temperature of blading materials. An investigation of the gas turbine thermodynamic cycle reveals the magnitude of improvement possible by increasing turbine operating temperatures. Thus an investigation conducted by the NACA (Ref. 1) shows that for a given mass flow of working fluid the specific power output is proportional and the specific fuel consumption is inversely proportional to the inlet temperature. Fig. 1 illustrates this relation.

The increase of turbine inlet temperature, however, is limited by high temperature strength of blade materials. The development of high temperature metals is proceeding, but at a slow rate. The slowly metallurgical progress has been made as shown in Fig. 80 of Ref. 2. Allowable blade temperatures advanced from 1400° F. in 1910 to 1500° F. by 1930 and to 1600° F. by 1946. The rate of increase has been no greater since 1946.

Non-metallic materials such as ceramics have yet to demonstrate their adaptability to the rigorous service

requirements of turbine blading. As a result the use of some method of cooling the gas turbine blading presents itself as the method of allowing higher gas temperatures with present materials.

Several methods of blade cooling have been proposed and evaluated. A discussion of these methods as related to this thesis follows.

Late model German turbojet engines such as the Jumo 004 employed hollow turbine blade cooled internally by means of air blown into the root and exhausted at the tip. 1650° F. turbine inlet temperature was used with 7% of compressor air output required to cool blades approximately 400° F.

The NACA has proposed (Ref. 1) an improvement to this method by inserting a core in the blade, leaving a small annular air passage. It was found that the heat transfer from blade to cooling air was principally in the boundary layer and adjacent cooling air so the insert permitted similar cooling with less air flow. Fig. 2 graphs the results of this improvement.

Another cooling method consists of circulating water through internal passages in the blade. This system of cooling has accomplished very large blade temperature reductions. German applications (Ref. 3) conducted by Dr. Schmidt permitted 850-930° F. blade temperatures with a gas temperature of 2200° F. Fig. 3 shows an NACA analytical

investigation of water cooling which also gave considerable blade temperature reduction. It must be pointed out that while water cooling is very effective, the problems of handling the high temperature, high pressure water flow at high rates makes service application of this method difficult.

A modification of the foregoing system, known as rim cooling, has also been tried. Here water is circulated through the rotor rim so as to extract heat from the blade root. Less temperature reduction is obtained and the disadvantages of the water coolant system still exist. Fig. 4 shows rim cooling effectiveness. It can be seen from the figure that having a blade material of high thermal conductivity, K_M, is essential to this method.

All of the foregoing methods employ the same basic principle of cooling. They do not inhibit the heat transmission to the blade, but do increase the internal conductivity, or removal of heat, thereby affecting cooling. The proposal of this thesis is to substitute a boundary layer of cool air over the blade's surface in order to inhibit the heat transmission from the hot gases to the blade.

A coating of high temperature ceramic of low conductivity would embody this same principle. Fig. 5 shows the effectiveness of ceramic coatings of various thicknesses. While this is a very promising field insofar as temperature of operation is concerned, the inherent defects of brittle-

investigation of water cooling which also gave considerable blade temperature reduction. It must be pointed out that while water cooling is very effective, the problems of handling the high temperature, high pressure water flow at high rates makes service application of this method difficult.

A modification of the foregoing system, known as rim cooling, has also been tried. Here water is circulated through the rotor rim so as to extract heat from the blade roots. Some temperature reduction is obtained and the disadvantages of the water cooled system still exist. Fig. 6 shows rim cooling effectiveness. It can be seen from the figure that making a blade material of high thermal conductivity, Cu, is essential in this method.

All of the foregoing methods employ the same basic principle of cooling. They do not inhibit the heat transmission to the blade, but do increase the internal conductivity, or removal of heat, thereby effecting cooling. The proposal of this thesis is to substitute a boundary layer of cool air over the blade's surface in order to inhibit the heat transmission from the hot gases to the blade.

A coating of high temperature ceramics of low conductivity would embody this same principle. Fig. 7 shows the effectiveness of ceramic coatings of various thicknesses. While this is a very promising field insofar as temperature of operation is concerned, the inherent defects of brittle-

ness, thermal shock sensitivity and low tensile strength have obviated service use of ceramic covered blading.

If a region of low thermal conductivity can be interposed between the gas and the blade, then the objective of blade cooling could be accomplished. The natural boundary layer on the blade is such a region. However, the natural boundary layer forms at the temperatures of the gas. In this experiment the use of relatively cool air from the engine compressor is suggested to form a lower temperature boundary layer.

The justification of this idea is based on one of the fundamental laws of heat transfer, Faurier's equation for conduction (Ref. 4). (Experience has shown radiation effects to be secondary). Stated mathematically for steady state conduction:

$$q = KA \frac{dt}{dx}$$

where q = rate of heat transfer.

K = coefficient of thermal conductivity.

A = crossectional area of path.

$\frac{dt}{dx}$ = temperature gradient in direction of heat flow per unit distance.

This law shows that for a given configuration the rate of heat transfer from gas to blade may be made by reducing K and/or $\frac{dt}{dx}$.

K for air is reduced by reducing temperature. This is shown mathematically from Suchens equation:

$$K = K_{32} \frac{492 + C}{T + C} \left(\frac{T}{492}\right)^{3/2}$$

where T = absolute temperature

C = constant (.0129 for air).

K_{32} = K at 32° F.

The temperature gradient from the boundary layer to blade, $\frac{dt}{dx}$, is reduced by the use of the cool air controlled boundary layer. In fact, the cool air boundary layer will at first be lower in temperature than the blade so that the blade will transfer heat to the boundary layer. However, the temperature gradient from the hot gas to the boundary layer would be increased so it would be rapidly heated. The optimum configuration might therefore require a series of bleeds from the blade so the average temperature of the layer along the blade would be minimized.

In the author's experience a controlled boundary layer has been successfully employed to cool a liquid rocket nozzle. In 1936 the author collaborated in the construction of a liquid rocket motor in which a boundary layer of coolant air bled into the nozzle enabled prolonged operation. The nozzle was of mild steel yet endured the very high temperature rocket exhaust gases better than any contemporary nozzles of superior materials.

TEST EQUIPMENT

Fig. 5 shows the complete test equipment layout schematically. The test blade was mounted in a closed test section supplied with hot gas from a single J-33 combustion chamber. Fig. 6 is a photograph of the test section mounted on the burner. Air was supplied to the burner from the compressor of a naturally aspirated Allison V-1710 engine, Fig. 7. The quantity of gas flow was regulated by throttling the Allison engine while its temperature was controlled by burner fuel pressure. The temperature of the blade was measured by two thermocouples. All control and measurement was done from the control panel adjacent to the gas turbine test cell. Fig. 8 is a photograph of the control panel. The air which formed the controlled boundary layer was supplied from the laboratory air main at regulated pressure. The quantity of cooling air was measured in a standard design sharp edged orifice meter, shown in Fig. 9.

The test blade was manufactured from a solid Juno 004 turbine blade. Availability was the reason for selection of this blade. The "tinidur" type alloy (30% nickel, 14% chrome, 1.75% titanium, 12% carbon, balance, iron) possessed very difficult machining properties and low thermal conductivity. The blade roots were cut off flat for convenient mounting and the tip shortened by 3/4 inch

TEST EQUIPMENT

Fig. 5 shows the complete test equipment layout schematically. The test blade was mounted in a closed test section supplied with hot gas from a single J-33 combustion chamber. Fig. 6 is a photograph of the test section mounted on the burner. Air was supplied to the burner from the compressor of a naturally aspirated Allison V-1710 engine, Fig. 7. The quantity of gas flow was regulated by throttling the Allison engine while its temperature was controlled by burner fuel pressure. The temperature of the blade was measured by two thermocouples. All control and measurements was done from the control panel adjacent to the gas turbine test cell. Fig. 8 is a photograph of the control panel. The air which formed the neutralized boundary layer was supplied from the laboratory air main at regulated pressure. The quantity of cooling air was measured in a standard design sharp edged orifice meter, shown in Fig. 9.

The test blade was manufactured from a solid J-33 turbine blade. Availability was the reason for selection of this blade. The "Nimonic" type alloy (80% nickel, 20% chrome, 1.75% titanium, 1% aluminum, balance iron) possessed very difficult machining properties and low thermal conductivity. The blade roots were cut off flat for convenient mounting and the tip shortened by 3/4 inch

because of space limitations in the test section.

For the first test, configuration A was manufactured. In this blade the cooling air supply hole was drilled up the blade from root to 1/4 inch of tip through the thickest section. This hole was .20 inch in diameter. The air bleed holes (1/16 inch) were drilled from blade surfaces joining the supply hole. They were placed at a 45 degree angle with blade surface. There were six bleed holes to each surface. The exits were ground out with a fish tail countersink pattern to distribute the bleed air spanwise. A .15 inch hole was drilled up the leading edge for location of the thermocouple tip at midspan. The trailing edge was too thin to permit similar treatment so a 3/32 inch hole was drilled chordwise at midspan to snugly hold a thermocouple bead. The thermocouple was lead in in a stainless steel tube one inch downstream and bent 90 degrees and cemented in the trailing edge hole. Figs. 12, 13 and 14 show the thermocouple mounting. Fig. 10 shows the A blade between a standard blade and a shortened standard blade. The boundary layer is introduced at approximately the 30% chord point.

Configuration B blade is shown in Fig. 11. The boundary layer air supply was introduced through a .15 inch drilled passage 1/4 inch behind the leading edge. A 60 degree included angle slot was milled down the length of the leading edge and 3/32 inch bleed holes drilled joining the

because of minor distortions in the test section.

For the first test, configuration 1 was manufactured. On this blade the cooling air supply hole was drilled up the blade from root to 1/4 inch of tip through the thickest section. This hole was .08 inch in diameter. The air bleed holes (1/16 inch) were drilled from blade surfaces joining the supply hole. They were placed at a 45 degree angle with blade surface. There were six bleed holes to each surface. The holes were ground out with a fish tail countersink pattern to distribute the bleed air spanwise. A .06 inch hole was drilled up the leading edge for location of the thermocouple tip at midspan. The trailing edge was too thin to permit similar treatment so a 1/32 inch hole was drilled chordwise at midspan to accept only a thermocouple bead. The thermocouple was lead in in a stainless steel tube and lead downstream and bent 90 degrees and cemented in the trailing edge hole. Figs. 10, 11 and 12 show the thermocouple mounting. Fig. 10 shows the 1 blade between a standard blade and a machined standard blade. The boundary layer is introduced at approximately the 20% chord point.

Configuration 2 blade is shown in Fig. 11. The boundary layer air supply was introduced through a .10 inch drilled passage 1/4 inch behind the leading edge. A 30 degree included angle slot was milled down the length of the leading edge and 1/32 inch bleed holes drilled joining the

supply passage. In this design the cooling enters the slot opposed by stagnation pressure and flows out of the slot on both edges, forming the boundary layer.

The test section consisted of the blade mounting block shown in Fig. 13, and two side plates made of six inch channel. The bottom was closed with a 1/2 inch plate so that the hot gases which entered at the top were constrained to exhaust through the open side. The entrance and exit dimension are 3.5 x 4.5 inches. Fig. 12 pictures the complete test section. Fig. 14 shows another view of the blade mounting block. The test blade is centrally located with two parallel mounted standard blades to guide the flow.

Temperatures of the test blade were measured by 20 gauge chromel-alumel thermocouples which read on a Brown recorder. The small size thermocouples provided fast response and use of standard sillimanite insulations in the blade. The insulators were ground slightly in diameter for mounting in blade. The thermocouple tips were firmly seated in 3/32 inch holes for maximum sensitivity to blade temperatures. The trailing edge thermocouple bead was buried completely to insure it would sense blade, rather than gas temperatures.

Compensated lead wires connected the thermocouples to the selector switch for the recorder to eliminate errors in readings by variation in ambient temperature. The gas

supply passage. In this design the cooling enters the slot exposed by atmospheric pressure and flows out of the slot at both edges, forming the boundary layer.

The test section consisted of the blade mounting block shown in Fig. 11, and two side plates made of six inch channel. The bottom was closed with a 1/4 inch plate so that the hot gases which entered at the top were constrained to exhaust through the open side. The entrance and exit dimensions are 2.0 x 4.0 inches. Fig. 12 pictures the complete test station. Fig. 14 shows another view of the blade mounting block. The test blade is centrally located with two partially mounted standard blades to guide the flow.

Temperatures of the test blade were measured by 30 gauge chromel-alumel thermocouples which read on a Brown recorder. The small size thermocouples provided fast response and use of standard sillimanite insulators in the blade. The insulators were ground slightly in diameter for mounting in blade. The thermocouple tips were firmly sealed in 1/32 inch holes for maximum sensitivity to blade temperatures. The trailing edge thermocouple was not buried completely to insure it would sense blade, rather than gas temperatures.

Compensated lead wires connected the thermocouples to the selector switch for the recorder to eliminate errors in readings by variation in ambient temperature. The gas

temperature entering the test section, T_4, was measured by a radiation shielded chromel-alumel thermocouple.

temperature entering the test section, T_i, was measured by a radiation shielded platinum-platinum rhodium thermocouple.

TEST PROCEDURE

The temperature of the test blade was read with and without cooling air flow under exactly similar flow conditions. This technique permitted comparison of the two temperatures obtained to show the blade reduction due to cooling air alone.

The Allison engine was first started and its speed set to obtain the desired flow rate of burner air. The flow rate was measured by means of the pressure drop across the orifice in the compressor inlet duct.

Next, combustion was initiated in the burner with the spark and acetylene flare and fuel pressure adjusted until desired gas temperature obtained. When conditions stabilized temperatures and pressures were recorded. During runs with cooling air, the flow rate was varied in increments of 1/10 inch of water and temperature recorded when stabilized.

In order to investigate the cooling effects over a broad range of gas velocities three settings of the Allison engine were used to give low, medium and high gas flow rates. However, the low flow rate is not included in this report as it was unrealistically low compared with actual turbine operation. The flow rate was below minimum idling rate for a J-33 engine.

TEST RESULTS

The results of the experiment are contained in tables I and II and the graphs, Figs. 16 through 19. The graphs are plotted to show temperature reduction versus weight of cooling air flow.

These graphs are similar in shape and show that the reduction in blade temperature was approximately twice as great in the leading edge as the trailing edge. This is to be expected because of the increase in boundary layer temperature resulting from heat transmission from the gas. Also, the thinness of the blade section near the trailing edge offers more resistance to heat flow internally.

The graphs also show that the temperature reduction rate is greatest (the slope is maximum) at low cooling air rates. This is evidence that the boundary layer is established at low flow rates and is effective in reducing heat transfer. Beyond a flow rate of .2 lb./min. most of the graphs become straight line functions. This apparently results from thickening of the boundary layer and shows the insulating effect is proportional to the thickness. This effect conforms with Fourier's law. The cooling effectiveness, particularly at low flow rates, is greater with this method than the method of Fig. 2.

To illustrate the cooling effectiveness consider the J-33 turbojet engine. Maximum cooling of 280 F. at 1600 F. gas temperature could be accomplished with only 2% of compressor air.

Configuration A produced more uniform results than those of configuration B, as can be seen by comparing Figs. 16 and 17 with 18 and 19. Configuration A curves plotted more parallel and gave results proportional to gas temperature, while configuration B curves intersect and are out of order with gas temperature increments. Configuration A probably gave more uniform boundary layer formation, since the flows were convergent rather than opposed. It was calculated that the stagnation point on the leading edge would fall in the milled slot so the cooling air would spill over both surfaces of the blade and form good boundary layers. From the non-uniform results at different flow rates stagnation point shifting may be indicated. Also, turbulence in the test section may have prevented uniform boundary layer formation and promoted mixing. It is believed that had the blade been manufactured with boundary layer control slots of the type used in airplane practice, much higher quality results would have been obtained. This type bleed was considered but discarded because of the machining problems, which would have required machining beyond shop capacity.

Uncontrollable variation in the speed of the Allison engine contributed to inaccuracy of data. A "hunting" of about fifty RPM occurred during much of the running, which produced 500 RPM variations in compressor speed. The variation in burner air flow caused drifting of gas temperatures.

Comparison of Figs. 16 with 17, and 18 with 19, shows cooling effectiveness variation with gas flow rate. Cooling effectiveness is greater at the lower flow rate. This is consistent with the laws of heat transmission by convection. The heat transfer from gas to blade increases with velocity.

From all graphs, the blade temperature reduction is shown to increase with gas temperature. This, also, is compatible with the laws of heat transfer, the $\frac{dt}{dx}$ term of Fourier's equation increases so more heat is transferred to the outer boundary layer. But, the heat transfer to the blade through the laminar sublayer is of such small magnitude that the net effect is greater blade temperature reduction.

CONCLUSIONS

In view of the limited scope of the experimental tests, no detailed quantitative conclusions can be drawn. However, the results obtained from the foregoing tests do support the following general conclusions:

1. The introduction of a boundary layer of relatively cool air on a turbine blade in a high temperature, high velocity gas stream inhibits the transmission of heat from the gas to the blade, more than through the natural boundary layer, and results in reduction of blade temperature.

2. The magnitude of the reduction in blade temperature is proportional to the weight flow of air introduced into the boundary layer up to the limit investigated of 2% of the gas flow in an equivalent full scale engine.

3. This method of blade cooling is feasible insofar as weight flow of cooling air required to accomplish useful blade temperature reduction is concerned.

TABLE I

OBSERVED TEST DATA

HIGH AIR FLOW RUNS

COMPRESSOR RPM - 24,000

— GAS TEMPS —

RUN 1 — CONFIGURATION A

COOLING AIR ΔP "H_2O	W_a	800°F T_{BLE}	T.R.	T_{BTE}	T.R.	1000°F T_{BLE}	T.R.	T_{BTE}	T.R.	1200°F T_{BLE}	T.R.	T_{BTE}	T.R.	1400°F T_{BLE}	T.R.	T_{BTE}	T.R.	1600°F T_{BLE}	T.R.	T_{BTE}	T.R.
0	0	785		785		995		995		1190		1195		1390		1390		1585		1585	
.1	.217	720	65	760	25	920	75	965	30	1110	80	1150	45	1255	135	1325	65	1440	145	1615	70
.2	.345	710	75	755	30	920	75	965	30	1070	120	1135	60	1255	135	1325	65	1440	145	1505	80
.3	.471	700	85	750	35	895	100	950	45	1050	140	1135	60	1220	170	1310	80	1385	200	1480	105
.4	.600	690	95	735	50	875	120	945	50	1030	160	1110	85	1200	190	1300	90	1350	235	1465	120
.5	.726	675	110	730	55	855	140	937	58	1015	175	1115	80	1185	205	1290	100	1335	250	1450	135
.6	.846	665	120	730	55	850	145	930	65	1015	175	1115	80	1160	230	1210	190	1320	265	1450	135

RUN 2 — CONFIGURATION B

COOLING AIR ΔP "H_2O	W_a	800°F T_{BLE}	T.R.	T_{BTE}	T.R.	1000°F T_{BLE}	T.R.	T_{BTE}	T.R.	1200°F T_{BLE}	T.R.	T_{BTE}	T.R.	1400°F T_{BLE}	T.R.	T_{BTE}	T.R.	1600°F T_{BLE}	T.R.	T_{BTE}	T.R.
0	0	755		755		945		975		1150		1150		1325		1330		1480		1475	
.1	.217	725	30	750	5	915	30	965	10	1080	70	1120	30	1300	25	1318	12	1350	130	1440	35
.2	.345	695	60	735	20	900	45	955	20	1075	75	1120	30	1230	95	1310	20	1330	150	1440	35
.3	.471	670	85	720	35	875	75	945	30	1042	108	1120	30	1200	125	1310	20	1310	170	1425	50
.4	.600	650	105	720	35	855	90	935	40	1035	115	1120	30	1160	165	1295	35	1300	180	1425	50
.5	.726	640	115	715	40	825	120	920	55	1000	150	1115	35	1135	190	1290	40	1270	210	1420	55
.0	.846					800	145	905	70					1110	215	1275	55	1255	225	1420	55

		800°F	1000°F	1200°F	1400°F	1600°F
P_f	PSI	67	76	84	96	107
W_f	lb/hr	74	93	107	129	146
$\Delta P_{B.A.}$	"hg	1.83	1.82	1.80	1.65	1.50
$W_{B.A.}$	lb/sec	2.85	2.845	2.83	2.71	2.59
P_3	"hg	14.8	15.0	16.1	17.1	16.8
P_{t3}	"hg	15.4	15.4	16.5	17.5	17.2
P_4	"hg	.72	.64	.60	.52	.50
P_{t4}	"hg	11.45	11.8	13.1	13.75	13.8
q	"hg	10.63	11.16	12.5	13.23	13.3
M_4		.731	.75	.795	.82	.823

TEMP: COOLING AIR - 80°F

AMBIENT (T. CELL) 120°F

PRESS: ATMOS - 29.82 "hg

AMBIENT (TEST CELL) - 29.50 "hg

TABLE II

OBSERVED TEST DATA

MEDIUM BURNER AIR FLOW RUNS

COMPRESSOR RPM- 13,250

— GAS TEMPS —

RUN 3 — CONFIGURATION A

COOLING AIR ΔP "H_2O	W_a	800°F T_{BLE}	T.R.	T_{BTE}	T.R.	1000°F T_{BLE}	T.R.	T_{BTE}	T.R.	1200°F T_{BLE}	T.R.	T_{BTE}	T.R.	1400°F T_{BLE}	T.R.	T_{BTE}	T.R.	1600°F T_{BLE}	T.R.	T_{BTE}	T.R.
0	0	777		765		945		1000		1175		1200		1370		1345		1535		1570	
.1	.217	720	57	750	35	912	83	963	37	1052	143	1135	65	1210	120	1338	51	1410	15	1550	40
.2	.345	710	67	750	35	815	100	950	50	1042	150	1121	73	1230	160	1325	70	1422	103	1540	50
.3	.471	645	82	750	35	860	135	940	60	1035	160	1120	80	1202	188	1312	83	1388	117	1550	40
.4	.600	685	72	750	35	850	145	940	60	1015	180	1120	60	1175	215	1303	72	1365	220	1550	40
.5	.726	610	101	750	35	835	160	940	60	1010	165	1120	50	1150	240	1300	75	1340	245	1550	40
.6	.846	655	122	750	35	825	170	940	60	985	210	1120	50	1135	255	1300	75	1315	270	1540	50
.7	.972	650	121	750	35	815	180	940	60	975	220	1120	50	1120	270	1300	75				
.8	1.09	645	132	750	35	800	175	930	70	965	230	1120	80								

RUN 4 — CONFIGURATION B

COOLING AIR ΔP "H_2O	W_a	800°F T_{BLE}	T.R.	T_{BTE}	T.R.	1000°F T_{BLE}	T.R.	T_{BTE}	T.R.	1200°F T_{BLE}	T.R.	T_{BTE}	T.R.	1400°F T_{BLE}	T.R.	T_{BTE}	T.R.	1600°F T_{BLE}	T.R.	T_{BTE}	T.R.
0	0	720		725		930		945		1142		1147		1325		1320		1490		1480	
.1	.217	645	75	706	11	860	170	930	15	1042	100	1120	21	1138	137	1265	35	1385	105	1455	25
.2	.345	640	80	700	25	850	130	925	20	1030	112	1120	21	1182	143	1235	65	1365	135	1455	25
.3	.471	632	88	700	25	831	133	925	20	1015	127	1110	37	1175	150	1275	45	1336	104	1450	30
.4	.600	625	95	700	25	825	205	925	20	1000	142	1100	41	1120	205	1270	50	1275	215	1438	42
.5	.726	605	115	695	30	800	230	915	30	965	111	1095	52	1108	217	1255	67	1250	240	1425	55
.6	.846	INSUFFICIENT COMPRESSED AIR SUPPLY																			
.7	.972																				
.8	1.09																				

		800°F	1000°F	1200°F	1400°F	1600°F
P_f	PSI	49	61	67	73	79
W_f	lb/hr	47	65	80	90	103
$\Delta P_{B.A.}$	"Hg	1.05	.95	.88	.83	.80
$W_{B.A.}$	lb/sec	2.16	2.06	1.48	1.42	1.89
P_3	"Hg	7.1	7.8	8.4	8.6	9.1
P_{T3}	"Hg	6.5	8.0	8.6	8.7	9.3
P_4	"Hg	.8	.55	.4	.32	.30
P_{t4}	"Hg	5.8	5.8	6.55	6.95	7.35
g	"Hg	5.0	5.25	6.15	6.60	7.05
M_4		.494	.500	.551	.595	.60

TEMPS: COOLING AIR 80°F
AMBIENT TEST CELL 120°F

PRESS: ATMOSPHERIC 29.82 "Hg
AMBIENT TEST CELL 29.50 "Hg

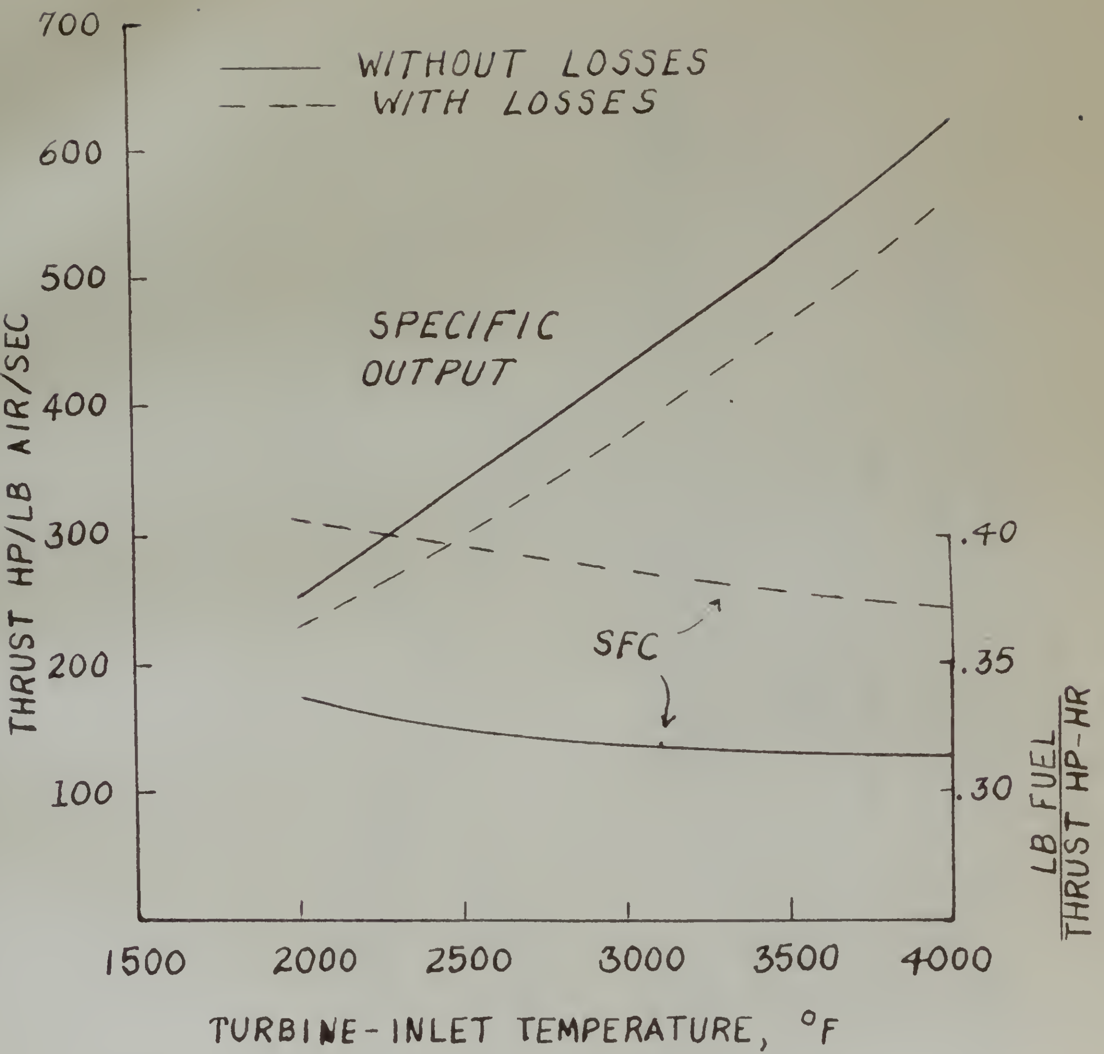

TURBOPROP ENGINE PERFORMANCE WITH +WITHOUT COOLING LOSSES. AIRPLANE SPEED, 500 MPH: MACH NO., 0.69; ALTITURE 30,000 FT. (Ref. 1)

Fig. 1

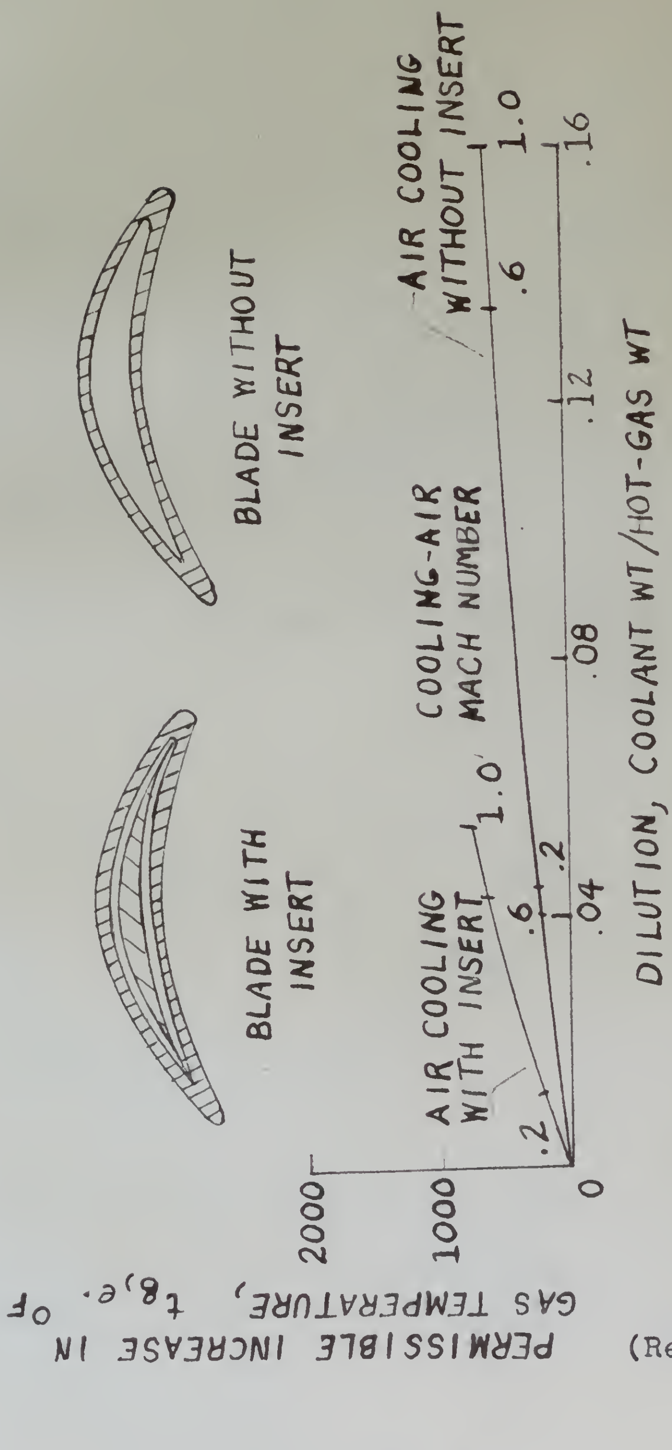

VARIATION OF PERMISSIBLE GAS TEMPERATURE INCREASE WITH DILUTION. LIFE, 1000 HRS.; BLADE MACH NO., 0.5

(Ref. 1)

Fig. 2

THERMAL CONDUCTIVITY, k_m, 15 BTU/(HR)(°F)(FT)

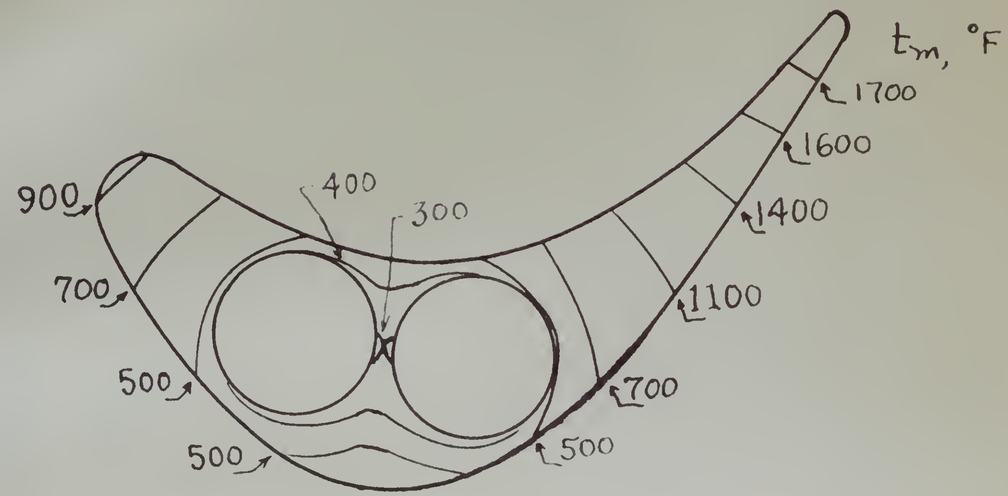

THERMAL CONDUCTIVITY, k_m, 100 BTU/(HR)(°F)(FT)

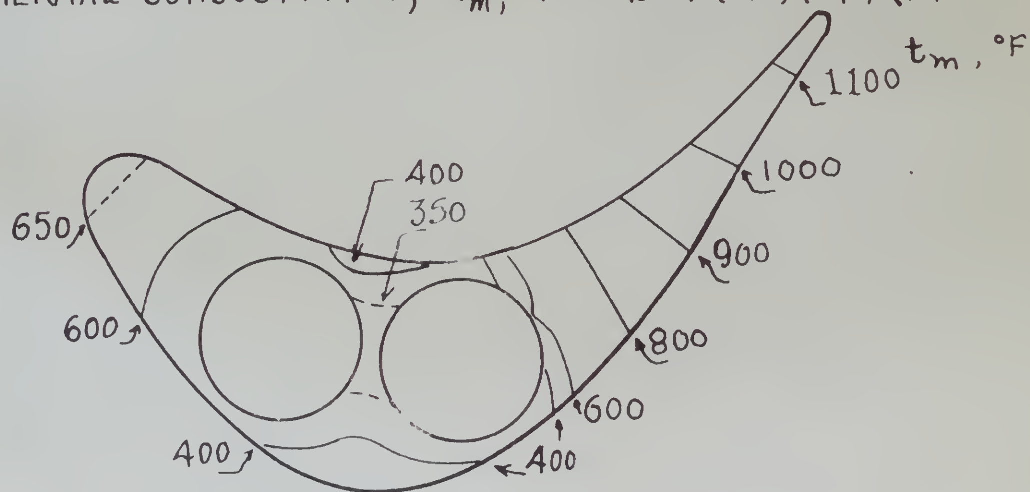

ISOTHERMS IN BLADE SECTIONS OF DIFFERENT CONDUCTIVITY MATERIAL WITH LIQUID COOLING. GAS FLOW, 55 LB/SEC; WATER FLOW, 6.42 LB/SEC; GAS TEMPERATURE, 2000° F; WATER TEMPERATURE, 200° F.
(Ref. 1)

Fig. 3

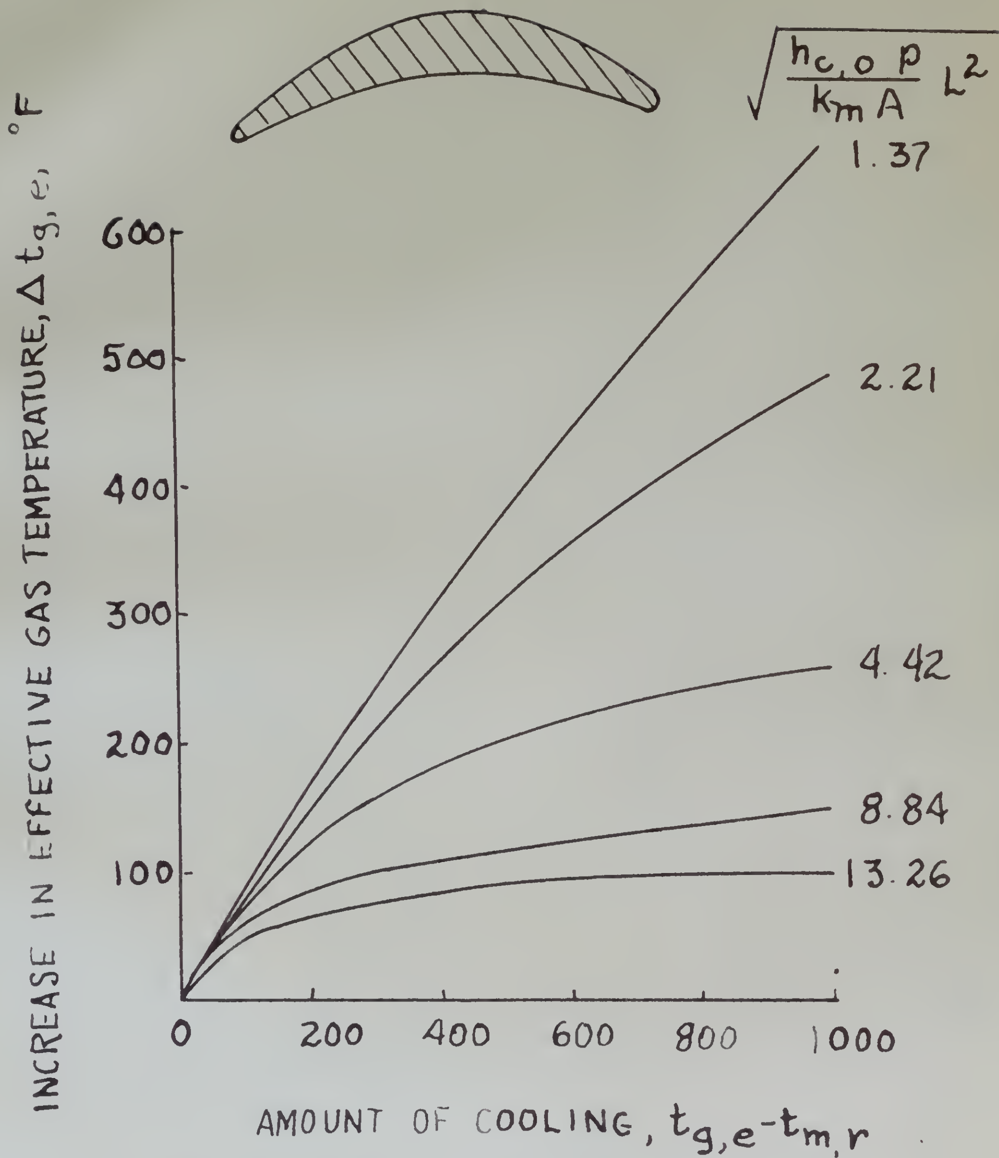

VARIATION OF RIM COOLING EFFECTIVENESS.
MAXIMUM ALLOWABLE MACH NUMBER, 0.5.
(Ref. 1)

Fig. 4

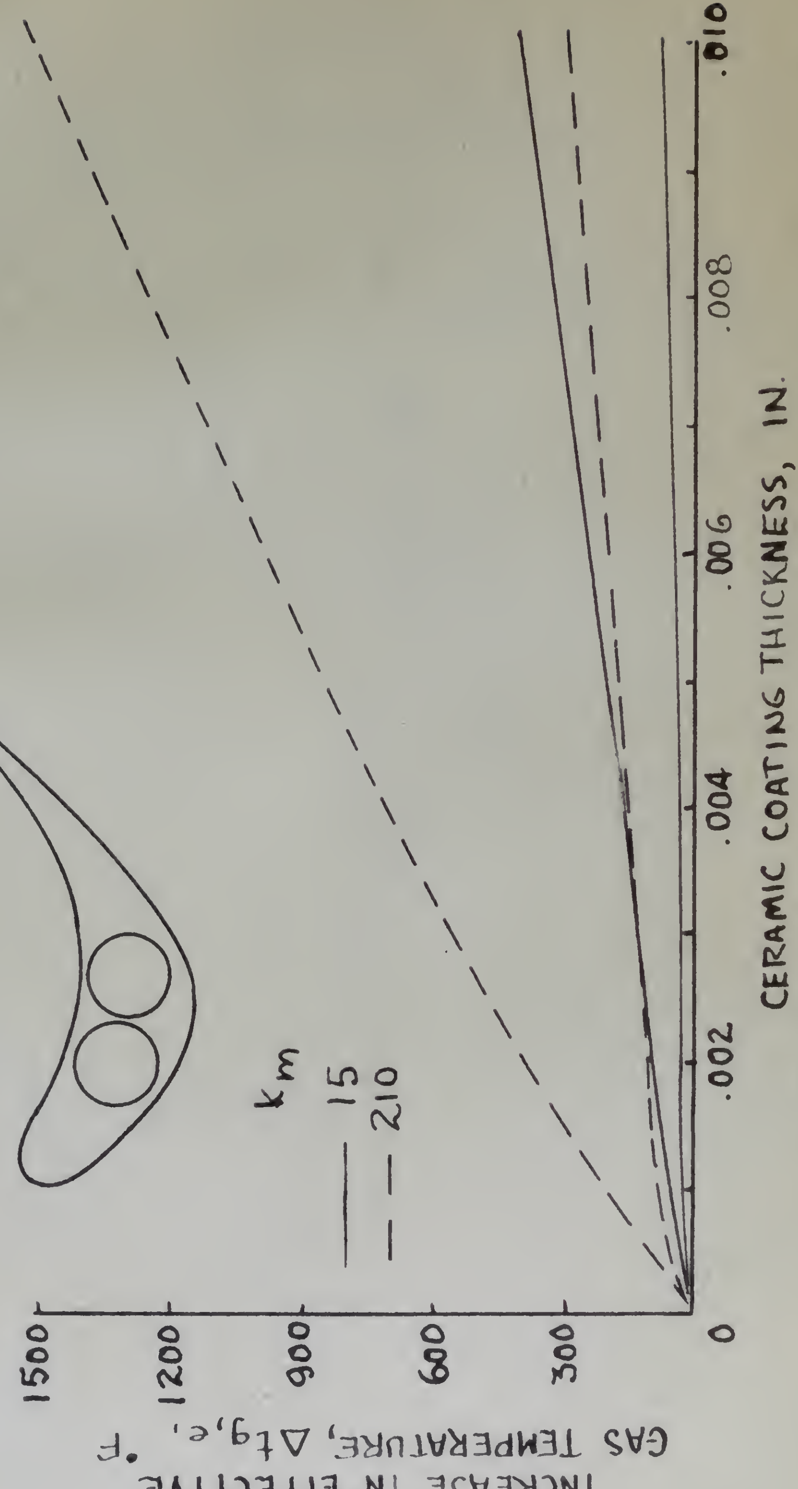

VARIATION OF INCREASE IN EFFECTIVE GAS TEMPERATURE WITH CERAMIC COATING THICKNESS FOR TWO METAL AND CERAMIC THERMAL CONDUCTIVITIES.

(Ref. 1)

Fig. 5

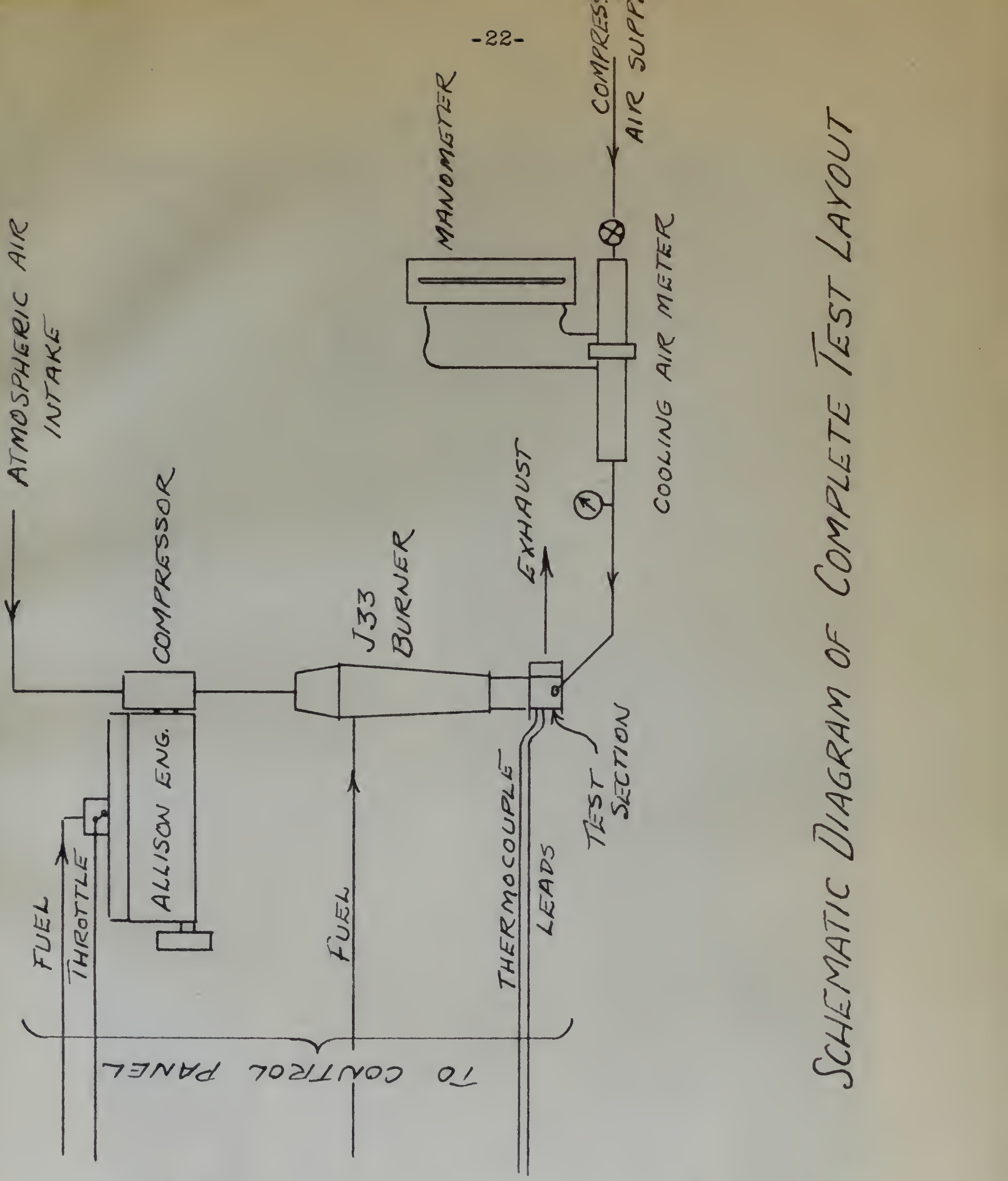
SCHEMATIC DIAGRAM OF COMPLETE TEST LAYOUT
ATMOSPHERIC AIR INTAKE
COMPRESSOR
ALLISON ENG.
FUEL
THROTTLE
J33 BURNER
FUEL
THERMOCOUPLE LEADS
TEST SECTION
EXHAUST
MANOMETER
COOLING AIR METER
COMPRESS AIR SUPP
TO CONTROL PANEL

Fig. 6

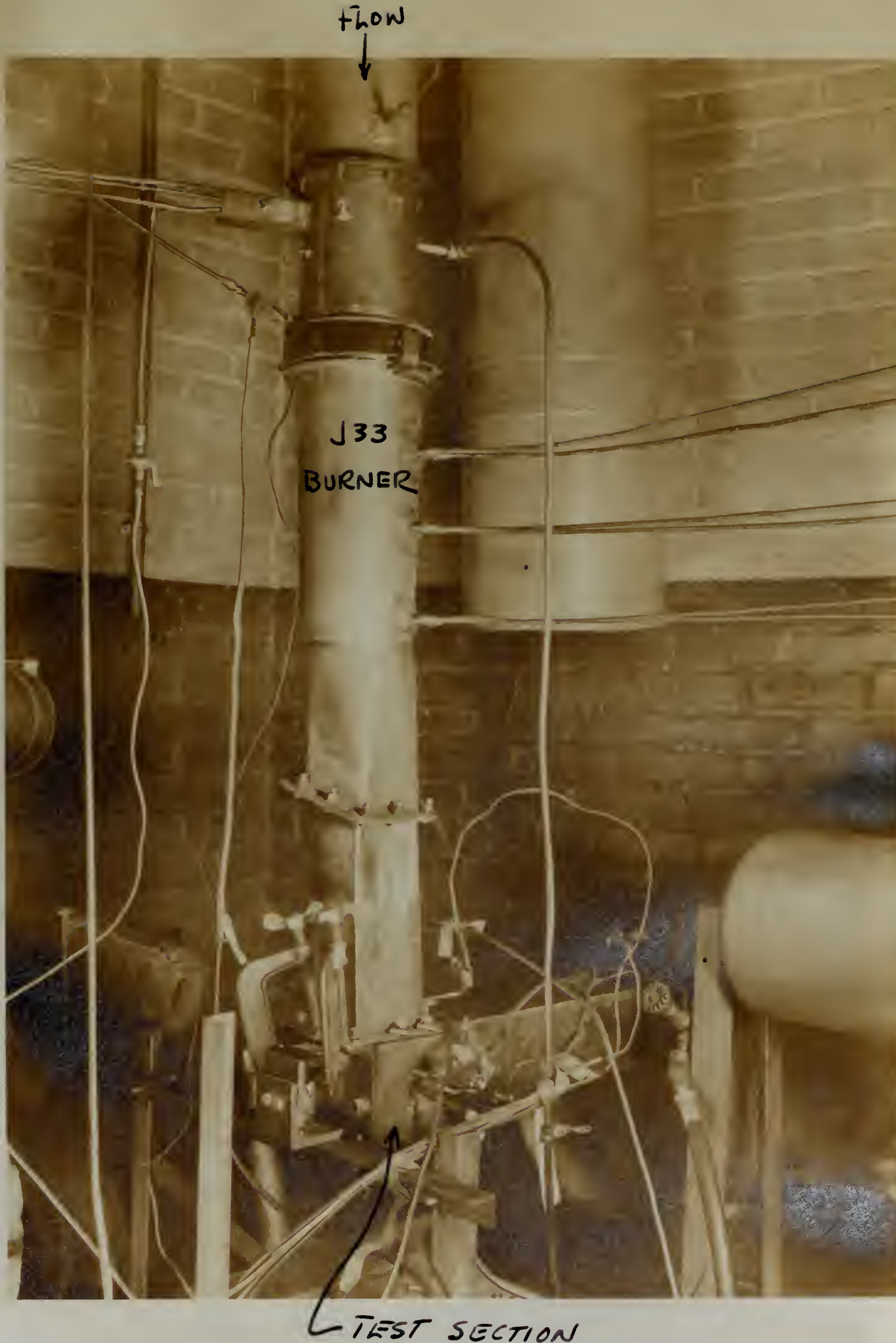

TEST SECTION MOUNTED ON BURNER

Fig. 7

ALLISON ENGINE

Fig. 8

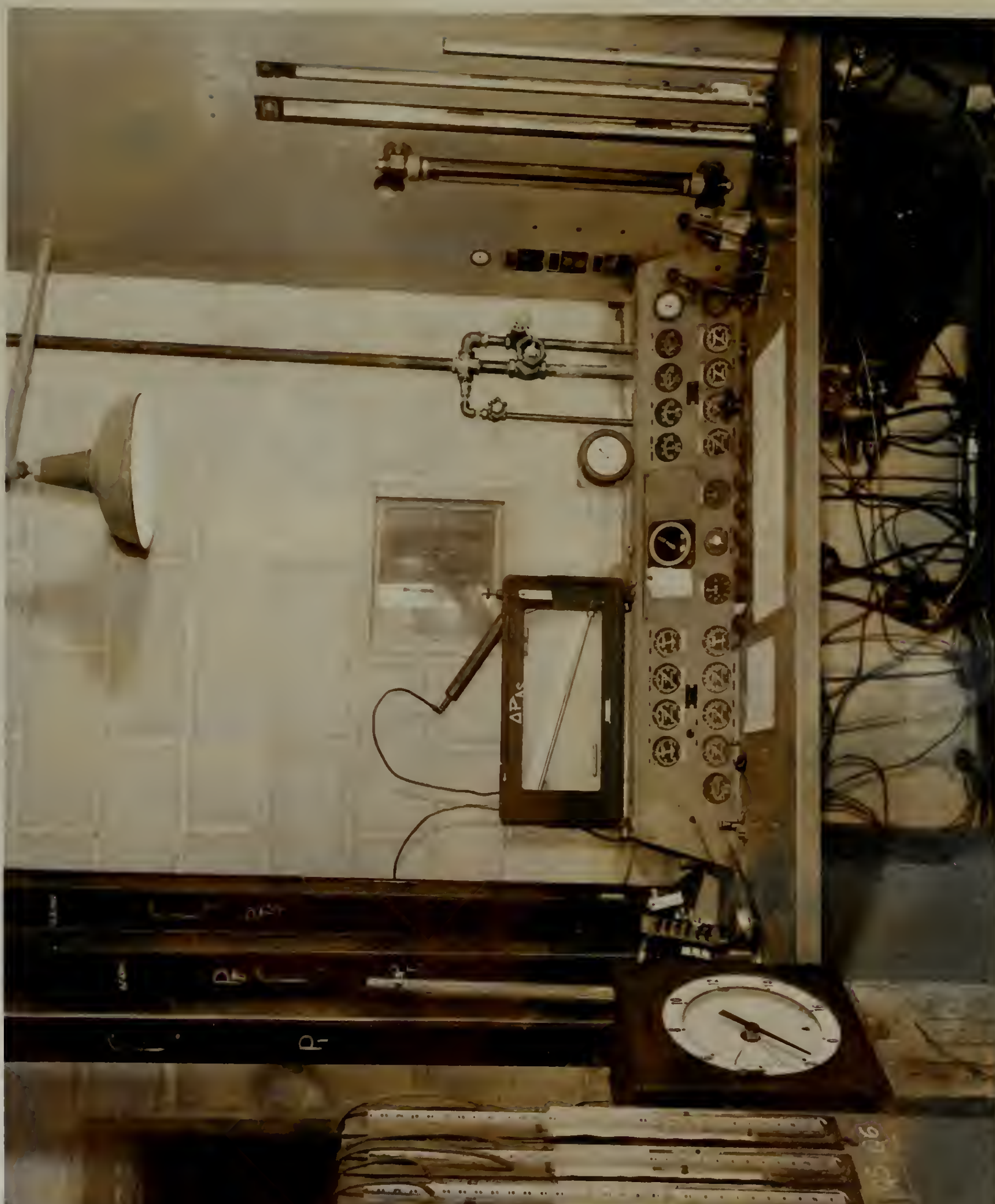

CONTROL PANEL

Fig. 9

COOLING AIR METER

Fig. 10

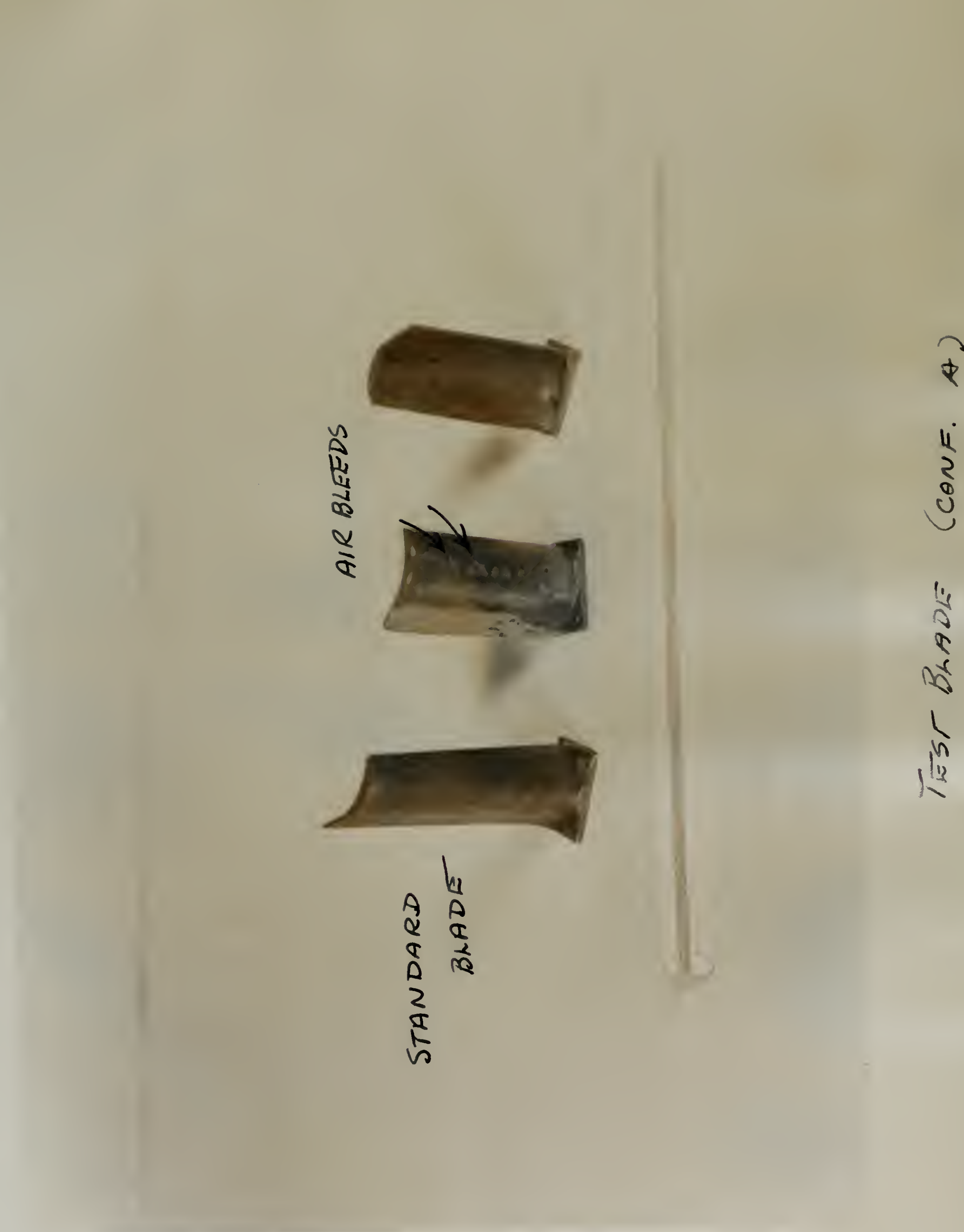

Fig. 11

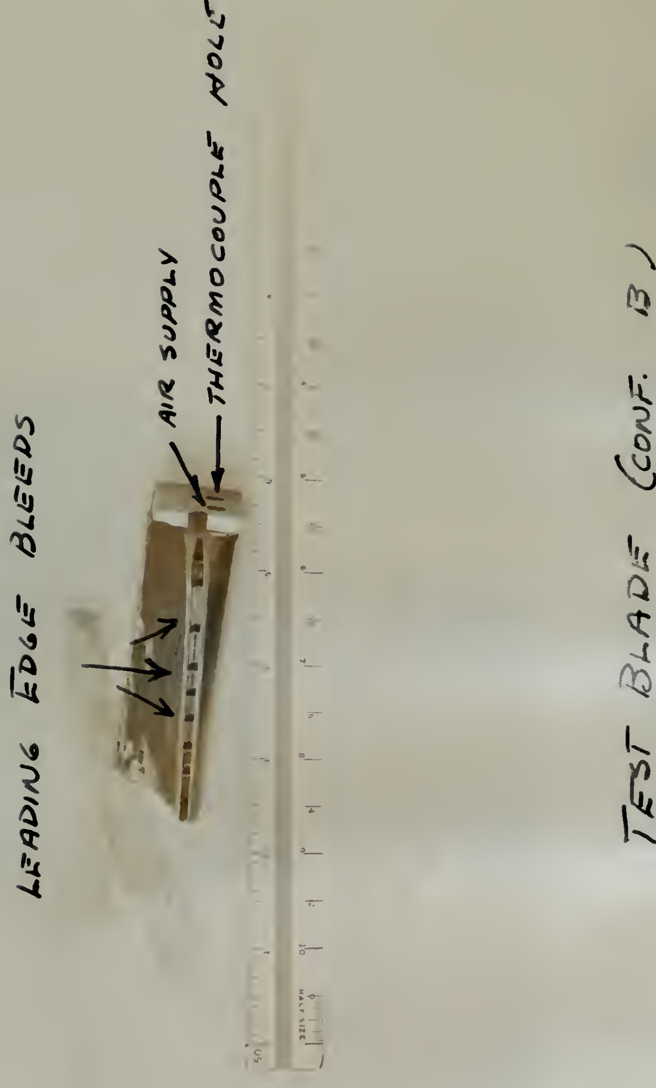

LEADING EDGE BLEEDS
AIR SUPPLY
THERMOCOUPLE HOLE
TEST BLADE (CONF. B)

Fig. 12

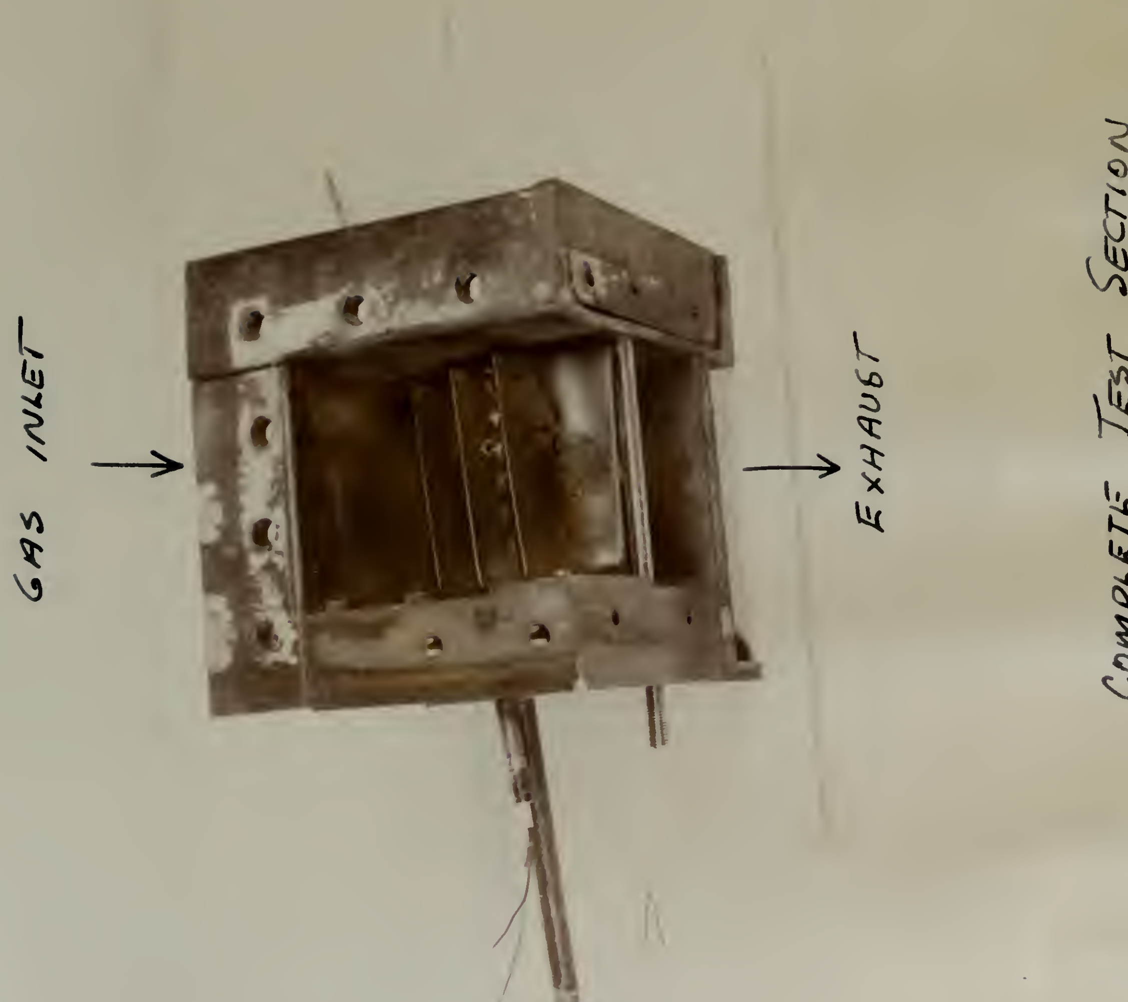

Fig. 13

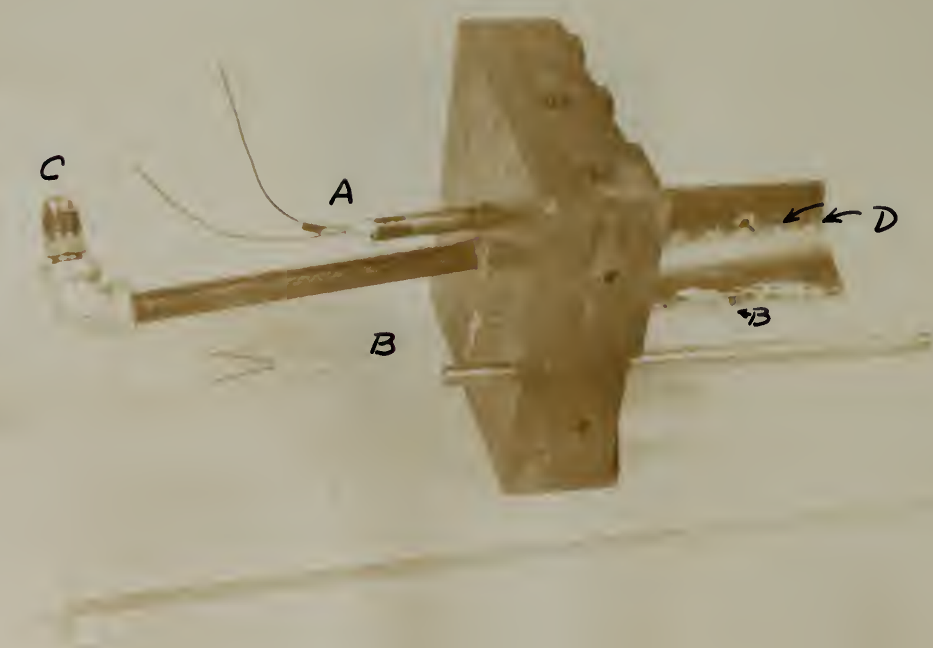

A - LEADING EDGE THERMOCOUPLE

B - TRAILING EDGE THERMOCOUPLE

C - COOLING AIR SUPPLY

D - " " BLEEDS

MOUNTED TEST BLADE

Fig. 14

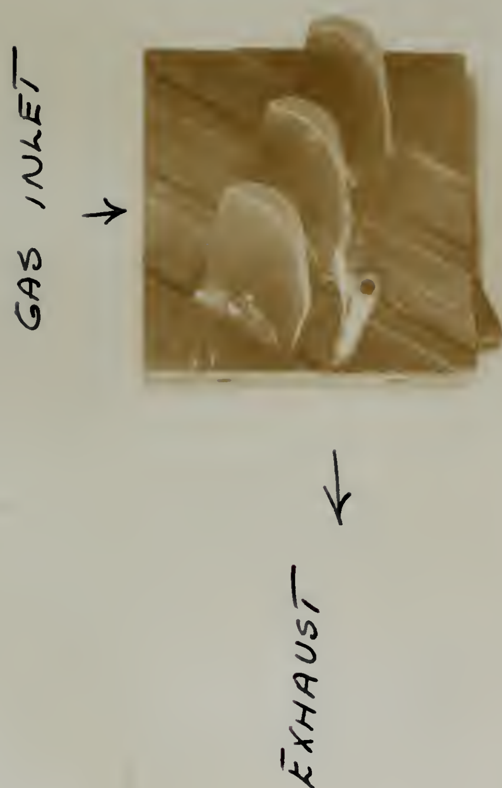

END VIEW OF BLADES

Fig. 15

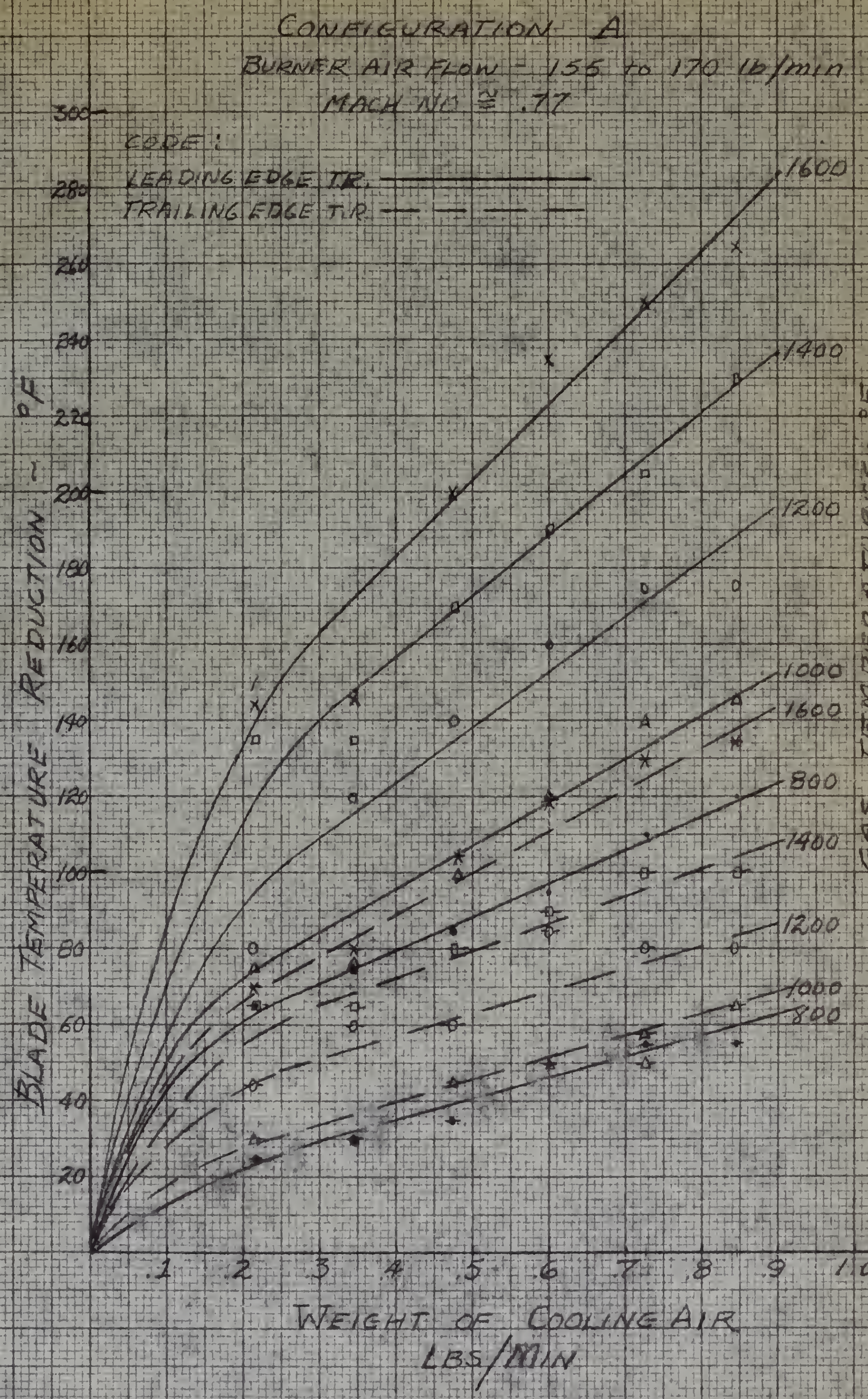
CONFIGURATION A
BURNER AIR FLOW - 155 to 170 lb/min
MACH NO ≅ .77
CODE:
LEADING EDGE T.R.
TRAILING EDGE T.R.
BLADE TEMPERATURE REDUCTION ~ °F
GAS TEMPERATURES ~ °F
1600
1400
1200
1000
1600
800
1400
1200
1000
800
300
280
260
240
220
200
180
160
140
120
100
80
60
40
20
.1
.2
.3
.4
.5
.6
.7
.8
.9
1.0
WEIGHT OF COOLING AIR
LBS/MIN

FIG. 16

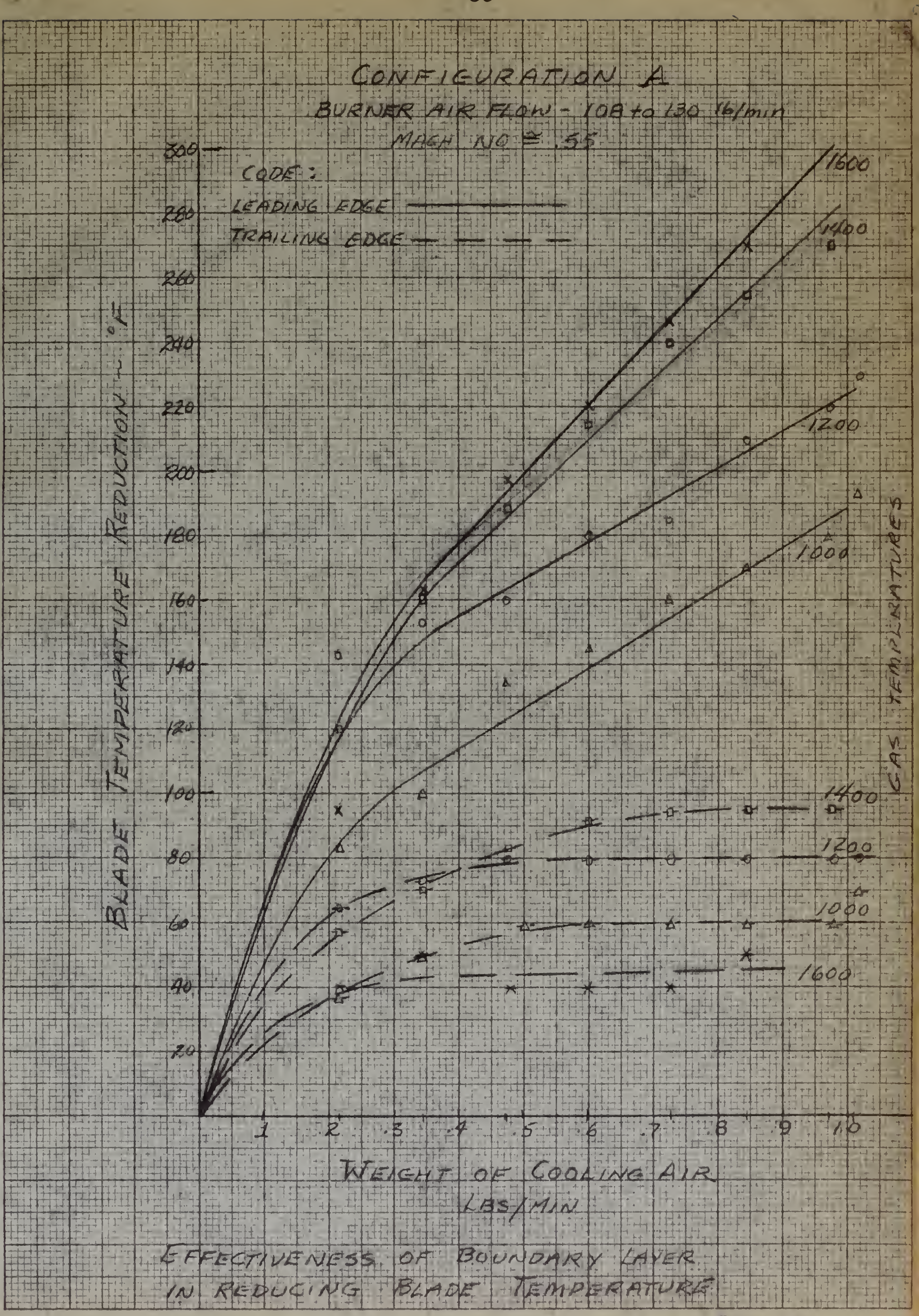
CONFIGURATION A
BURNER AIR FLOW - 108 to 130 lb/min
MACH NO ≅ .55
CODE:
LEADING EDGE
TRAILING EDGE
BLADE TEMPERATURE REDUCTION ~ °F
300
280
260
240
220
200
180
160
140
120
100
80
60
40
20
.1
.2
.3
.4
.5
.6
.7
.8
.9
1.0
1600
1400
1200
1000
1400
1200
1000
1600
GAS TEMPERATURES
WEIGHT OF COOLING AIR
LBS/MIN
EFFECTIVENESS OF BOUNDARY LAYER
IN REDUCING BLADE TEMPERATURE

Fig. 17

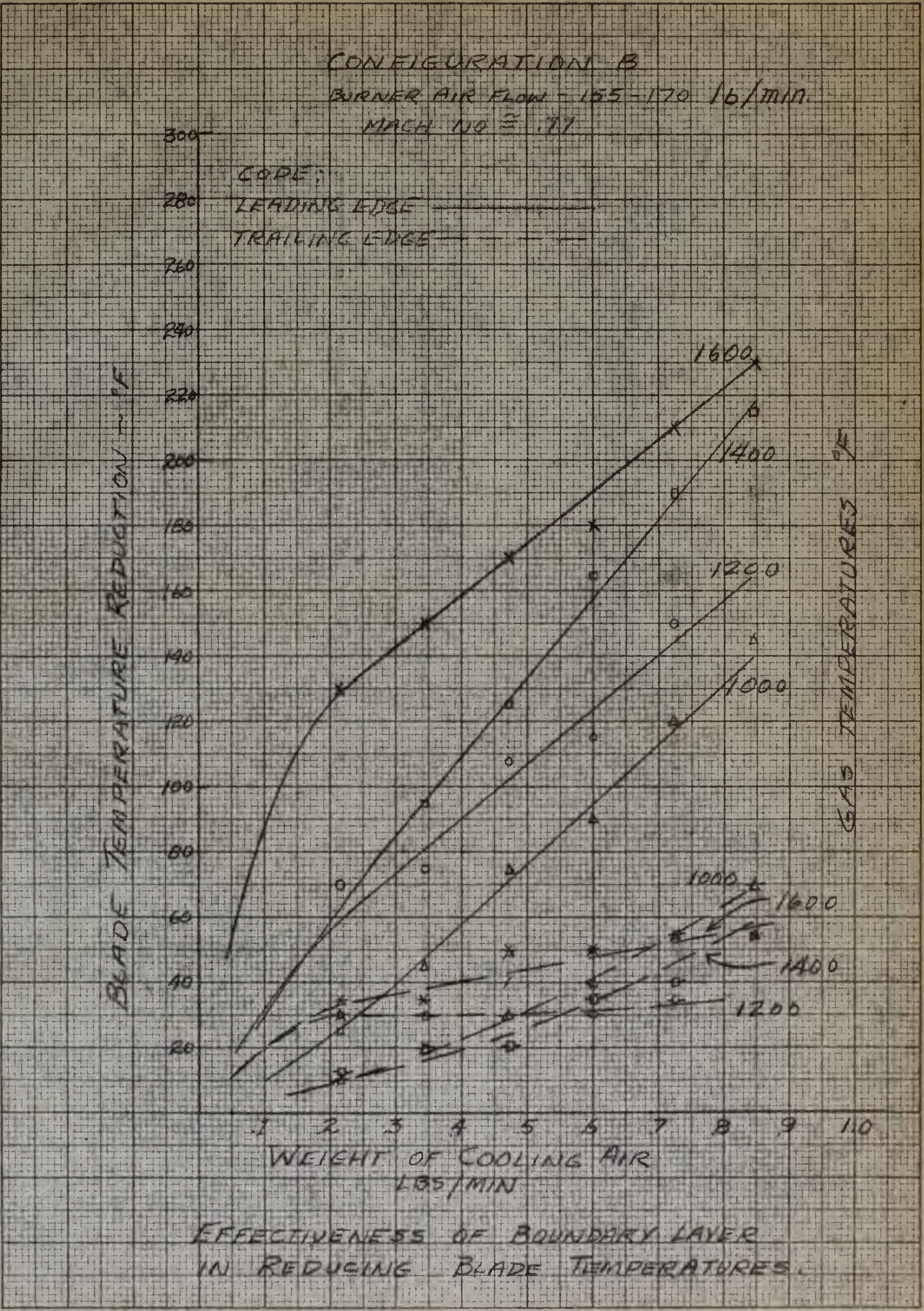

EFFECTIVENESS OF BOUNDARY LAYER IN REDUCING BLADE TEMPERATURES.

Fig. 18

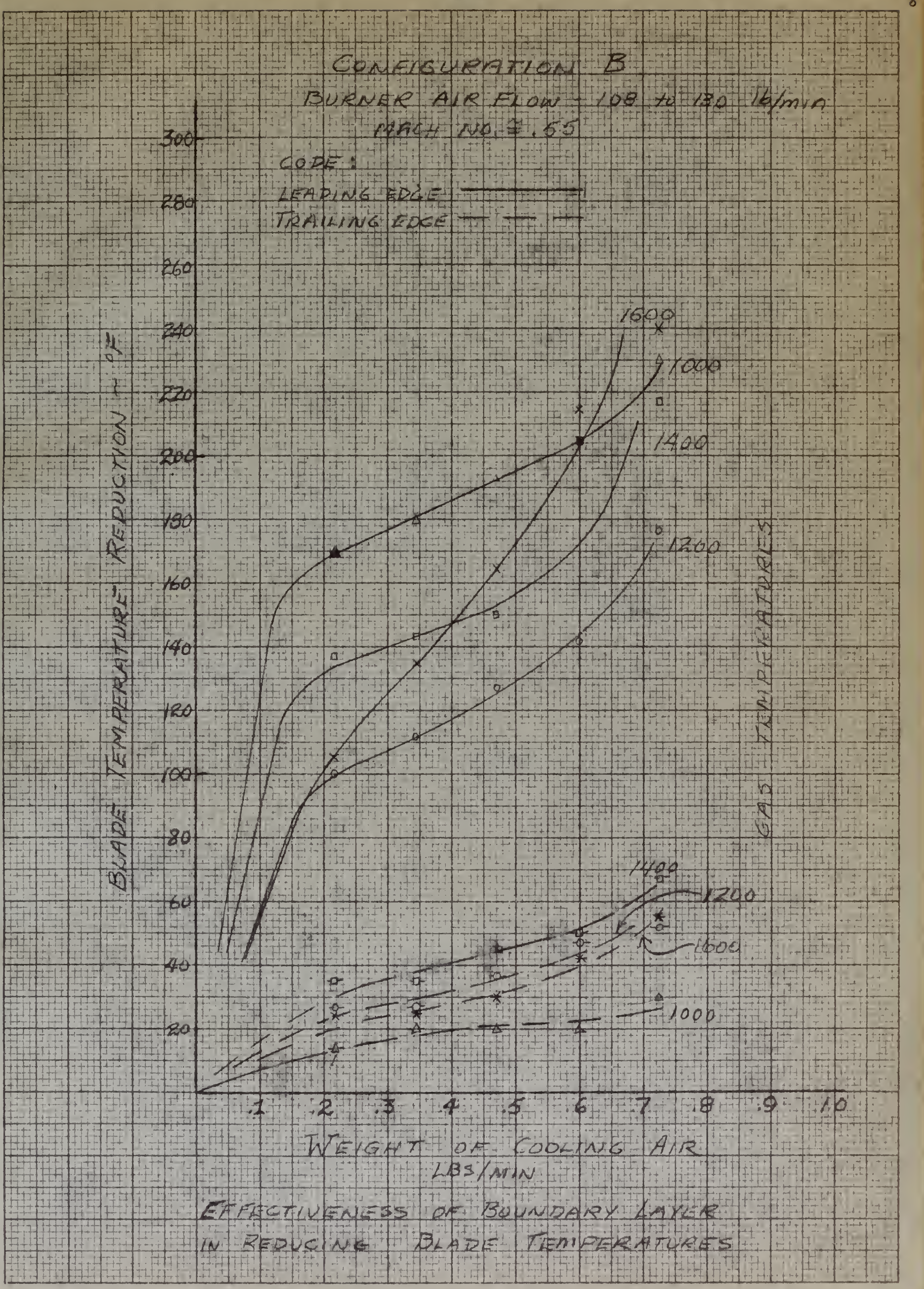
CONFIGURATION B
BURNER AIR FLOW - 108 to 130 lb/min
MACH NO. ≅ .65
CODE:
LEADING EDGE
TRAILING EDGE
BLADE TEMPERATURE REDUCTION ~ °F
GAS TEMPERATURES
1600
1000
1400
1200
1400
1200
1600
1000
300
280
260
240
220
200
180
160
140
120
100
80
60
40
20
.1
.2
.3
.4
.5
.6
.7
.8
.9
1.0
WEIGHT OF COOLING AIR
LBS/MIN
EFFECTIVENESS OF BOUNDARY LAYER
IN REDUCING BLADE TEMPERATURES

Fig. 19

NOMENCLATURE

P_f	FUEL PRESSURE	psig
P_3	BURNER INLET STATIC PRESS	" Hg
P_{t_3}	" " TOTAL "	" Hg
P_4	TEST SECTION STATIC "	" Hg
P_{t_4}	" " TOTAL "	" Hg
ΔP_{CA}	COOLING AIR ORIFICE PRESS DROP	" H_2O
ΔP_{BA}	BURNER " " " "	" Hg
q	DYNAMIC PRESS	" Hg
M_4	TEST SECTION MACH NO.	
T	TEMPERATURE	°F

SUBSCRIPTS:

- B_{LE} BLADE LEADING EDGE
- B_{TE} " TRAILING "
- m, r " ROOT
- g, e GAS, AFFECTING HEAT TRANSFER

T.R.	TEMPERATURE REDUCTION	°F
w	WEIGHT FLOW	

SUBSCRIPTS:

CA	COOLING AIR	lb/min
BA	BURNER "	lb/sec
f	" FUEL	lb/hr

BIBLIOGRAPHY AND REFERENCES

(1) Ellerbrock, H. H.; "NACA Investigations of Gas Turbine Blade Cooling;" I. Ae. Sc. Reprint #117.

(2) Smith, G. G.; "Gas Turbines and Jet Propulsion for Aircraft," 4th Ed., Aircraft Books, Inc. 1946.

(3) Stewart, R. W.; "Literature Survey on the Use of Ceramic Materials for Turbine Blading." Allis-Chalmers Manufacturing Co., Turb-Power Development Department Report, 18 March, 1948.

(4) McAdams, W. H.; "Heat Transmission;" 2nd Ed., McGraw-Hill Book Co., 1942.

SAMPLE CALCULATIONS

Air metering: With standard sharp edged orifice configuration with flange taps.

Cooling air,

$$W_a = .8595\ K\ D_2^{\,2} \frac{(P_2\ .\ \Delta P)^{\frac{1}{2}}}{(T_a)^{\frac{1}{2}}} \quad \text{(ASME Power Test Code)}$$

T_a =	80° F.	Air supply temperature
D_2 =	.75"	Orifice diameter
D_1 =	2.07"	Pipe diameter
K =	.61	From Fig. 34(a) of ASME Power Test Codes
P_2 =		Absolute outlet static pressure lb./in.^{2}
ΔP =		Orifice static pressure drop lb./in.^{2}

$$W_a = \frac{.8596 \times .61 \times (.75)^2}{(540)^{\frac{1}{2}}} (P_2 \times \Delta P)^{\frac{1}{2}}$$

$$= .01268\ (P_2 \times \Delta P)^{\frac{1}{2}}$$

P	P(psi)	P_2	W_a(lb./sec.)	W_a(lb./min.)
.1	.0036	22.6	.00362	.217
.2	.0072	28.6	.00575	.345
.3	.0108	35.6	.00785	.471
.4	.0144	43.6	.01	.60
.5	.0180	50.6	.0121	.726
.6	.0216	57.6	.0141	.846
.7	.0252	64.6	.0162	.972
.8	.0288	71.6	.0182	1.09

Burner air,

$$W_{BA} = .8596\ K\ D_2^2 \frac{(P_2 \times \Delta P)^{\frac{1}{2}}}{T_1^{\frac{1}{2}}}$$

K = .704

D_2 = 5.6

Results are tabulated in Tables I and II.

Mach. number:

$$q = \frac{\gamma}{2} P M^2$$

M_4 = Test section mach. no.

q = Test section dynamic pressure

γ = 1.3 for gas

P_4 = Test section static pressure

$$M_4 = \frac{2q}{\gamma P_4} = \frac{q}{.65 P_4}$$

Results are tabulated in Tables I and II.

Thesis 11472
N4 Ness

Boundary layer control as a method of gas turbine blade cooling.